

The Diffractive Process in Six-Prong Proton-Proton Interactions
at 205 GeV/c*

P. F. SCHULTZ, M. DERRICK, B. MUSGRAVE,
P. SCHREINER, and H. YUTA

Argonne National Laboratory, Argonne, Illinois 60439

We have studied the 6-prong events in a 50,000 picture exposure of the 30-inch bubble chamber to a 205 GeV/c proton beam at the Fermi National Accelerator Laboratory. The data consists of complete measurements of 446 events containing a proton track with $P_{\text{Lab}} < 1.4 \text{ GeV/c}$ identified by ionization. A low mass diffractive peak is clearly seen in the events with 5 charged particles in the forward CM hemisphere. An analysis based on the rapidity distributions of the outgoing tracks and the missing mass gives a single diffractive cross section of $0.38 \pm 0.05 \text{ mb}$, of which a quarter corresponds to the 4-constraint events $pp\pi^+\pi^+\pi^-\pi^-$. In the diffractive sample, only $0.1 \pm 0.03 \text{ mb}$ corresponds to events decaying through a Δ^{++} intermediate state. Comparing this data to the low mass enhancements seen in the 2- and 4-prong data in our experiment, one finds a systematic variation of the diffractive peak position with particle number.

The United States and the Atomic Energy Commission, nor any of their employees, their contractors, subcontractors, agents, or assigns, makes any warranty, express or implied, or assumes any legal liability or responsibility for the accuracy, completeness or usefulness of any information, apparatus, product or process disclosed, or represents that its use would not infringe privately owned rights.

*Work supported by the U. S. Atomic Energy Commission.

Introduction

Studies of the inclusive proton reaction



have been made over a wide range of energies⁽¹⁾ and show a low mass peak in the missing mass squared M_x^2 distribution. In our experiment at 205 GeV/c in the 30-inch HBC at the Fermi National Accelerator Laboratory, it was found that only the low multiplicity events (2-, 4-, and 6-prongs) contribute⁽²⁾ to this diffractive enhancement. Detailed studies^(3,4) of the 2- and the 4-prong events show that their single diffractive contributions to the low mass peak are 2.05 ± 0.22 mb and 2.38 ± 0.16 mb, respectively. In the 4-prong events, 25% of the low mass peak was found to come from the $pp\pi^+\pi^-$ final state with the remainder being contributed from states with 3 or more pions. The 6-prong events were estimated to contribute $10 \pm 3\%$ to the diffraction or 0.52 ± 0.18 mb. All these numbers are quoted for both CM hemispheres.

In this paper we report on our study of the complete 6-prong events and on their contribution to the low mass peak of reaction (1). Previously, only the slow proton was measured; no information was obtained about the individual make-up of the system X^+ apart from its charged particle multiplicity dependence. In the current study, we measured all outgoing tracks for those 6-prong events, in a given fiducial region, which had a proton with laboratory momentum less than 1.4 GeV/c. Each event was examined by a physicist and when possible, mass assignments were made for the other 5 tracks on the

basis of observed ionization. Our present sample consists of 446 events corresponding to a microbarn equivalent of $6.06 \mu\text{b}/\text{event}$.

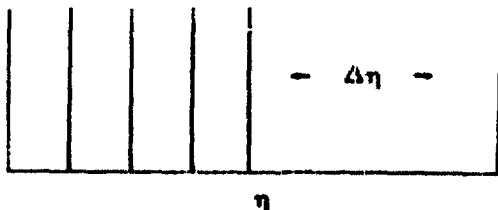
Results

We first present the evidence for diffractive dissociation of the beam particle. Fig. 1(a) shows the square of the missing mass, MM^2 , of the system recoiling from the slow proton. In Fig. 1(b-f) we show this MM^2 distribution separated according to the number of charged particles in the forward CM hemisphere. We refer to events with i charged particles in the forward CM hemisphere and j charged in the backward CM hemisphere as " (i, j) " events. We note that the events with low MM^2 are almost all from the $(5, 1)$ events, with only a small contribution from the $(4, 2)$ events.

To continue the analysis, we consider the particle distributions in the ordered rapidity chain. For convenience, we use the pseudo-rapidity variable

$$\eta = \ln(\tan \theta / 2) , \quad (2)$$

where θ is the laboratory production angle for an outgoing particle. For those events in which the beam particle diffractively dissociates, we expect the recoiling target proton to be well separated from the remaining particles in the ordered rapidity chain as shown below.



In our study of the diffractive process in the 4-prong events, this technique was used and a minimum rapidity gap $\Delta\eta = 2.5$ was found appropriate to define diffraction. Fig. 2 shows the MM^2 distribution for the 6-prong events which have a proton on the end of the rapidity chain and for which the largest η gap is also the first gap (the gap on the right in the above diagram). Comparing this to Fig. 1(a), one notes that almost all the events with $MM^2 < 40 \text{ GeV}^2$ appear in Fig. 2. The cross-hatched part corresponds to the events for which the first gap is greater than 2.5 units. For these events, the average η of the five particles is -4.6 units and the average spread in η per event is 2.3 units. Using the same definition as was previously used for the 4-prong events, we find 64 events having $\Delta\eta > 2.5$ units in the shaded distribution with $MM^2 < 40 \text{ GeV}^2$. This corresponds to a single diffractive cross section of $0.38 \pm 0.05 \text{ mb}$ for one CM hemisphere. Our definition of diffraction using the rapidity gap and MM^2 selections allows for some pions to 'leak' into the backward hemisphere. We may compare this number to the diffractive cross section of $0.26 \pm 0.09 \text{ mb}$ estimated from an analysis of the MM^2 distribution only. (2)

To estimate the contribution to the peak from the reaction

$$pp \rightarrow pp\pi^+\pi^+\pi^-\pi^-, \quad (3)$$

we have fitted the 6-prong events with the kinematic fitting program SQUAW and looked for 3- or 4-constraint fits. Since we are interested in fits for which a proton is the fastest particle in the lab frame, we accepted only those fits for which the fast forward proton had laboratory momentum $> 150 \text{ GeV}/c$.

Studies of the positive pion X distribution (where X here is the Feynman variable) show very few events with $|X| > 0.6$, and so we have also used a π^+ laboratory momentum $< 110 \text{ GeV}/c$ ($\equiv X < 0.6$) selection. The mass assignments to the tracks also have to agree with the observed track ionization. In Fig. 2(b) we show the distribution in MM^2 from the slow proton for the events with accepted fits to reaction (3), and for which the largest η gap is the first gap. This may be compared to the distribution for events which satisfy our criteria for diffraction shown in Fig. 2(a). Fig. 2(c) shows those diffractive events which do not have accepted fits to reaction (3). Note that the peak is at a higher value of MM^2 than for the events assigned to reaction (3). This agrees with earlier observations that the diffractive peak moves up in MM^2 as the number of constituent particles increases. ⁽⁴⁾ The results are summarized in Fig. 3, which shows the position of the diffractive peak for various topologies and number of final state particles and also in Table I.

In a companion study, ⁽⁵⁾ we have looked at the characteristics of inclusive Δ^{++} production. One interesting question is the extent to which the Δ^{++} results from the decay of a higher mass diffractively produced state. Since the Δ^{++} inclusive cross section is about equal to the diffractive cross section for the 6-prong events, this topology is critical for a study of the connection between diffraction and Δ^{++} production.

To investigate this question, we have chosen the events that are symmetric in the CM system to the (5, 1) events of Fig. 1. In Fig. 1 we see that there are only 41 (1, 5) events present, whereas we observe 85 (5, 1) events.

This implies that about half of the (5, 1) events contain a neutron (or perhaps a fast proton) in the final state.

Fig. 4(a) shows the $p\pi^+$ mass distribution for the (1, 5) events for which the target has diffracted. A clear peak corresponding to Δ^{++} production is observed. This peak of 18 events gives a cross section of 0.1 ± 0.03 mb, which may be compared both to the diffractive 6-prong cross section of 0.38 ± 0.05 mb and to the inclusive 6-prong Δ^{++} cross section of 0.40 ± 0.05 mb. Thus, there is only about a 25% overlap between diffraction and Δ^{++} production for the 6-prong topology.

References

1. See, for example, Proceedings of Vanderbilt Conference, Experiments on High Energy Particle Collisions 1973, AIP Conference Proceedings No. 12, Particle and Fields Subseries No. 4.
2. S. J. Barish et al., Phys. Rev. Lett. 31, 1080 (1973).
3. S. J. Barish et al., Phys. Rev. D9, 1171 (1974).
4. M. Derrick et al., Phys. Rev. D9, 1215 (1974) and ANL/HEP 7356, to be published in Phys. Rev. D.
5. S. J. Barish et al., "Study of the Reaction $p + p \rightarrow \Delta^{++} + X^0$ at 205 GeV/c," ANL/HEP 7427, paper submitted to this conference.

Table I
 Properties of the Low Mass Diffractive Enhancement in
 $pp \rightarrow pX$ at 205 GeV/c

Reaction	Approximate MM^2 Peak Position GeV^2	Cross Section mb	Composition of Final State
2-prong inelastic	2	1.02 ± 0.11	$N + \geq 1\pi$
4-prong 3C-4C fits	4.5	0.32 ± 0.07	$p\pi^+\pi^-$
remaining 4-prongs	10	0.86 ± 0.08	$N \geq 3\pi$
6-prongs 3C-4C fits	15	0.18 ± 0.04	$p\pi^+\pi^+\pi^-\pi^-$
remaining 6-prongs	35	0.21 ± 0.04	$N \geq 4\pi$

Figure Captions

Fig. 1 Missing mass squared (MM^2) distributions for the system recoiling from the slow proton in 6-prong events: (a) all events, (b) 85 events with 5 particles in the forward CM hemisphere, (c) 108 events with 4 particles in the forward CM hemisphere, (d) 131 events with 3 particles in the forward CM hemisphere, (e) 77 events with 2 particles in the forward CM hemisphere, and (f) 41 events with 1 particle in the forward CM hemisphere.

Fig. 2 Missing mass squared (MM^2) recoiling off the slow proton for those events with the proton on the end of the ordered rapidity chain and for which the largest rapidity gap is the one separating the proton from its nearest neighbor: (a) all events, (b) events giving acceptable fits to the reaction $pp \rightarrow pp\pi^+\pi^+\pi^-\pi^-$, (c) remaining events, i. e. the difference between (a) and (b).

Fig. 3 Missing mass squared distribution for the system recoiling from the slow proton for (a) the inelastic 2-prong events, (b) the (3, 1) 4-prong events fitting $pp \rightarrow pp\pi^+\pi^-$, (c) the remaining 4-prong events, (d) the (5, 1) 6-prong events fitting $pp \rightarrow pp\pi^+\pi^+\pi^-\pi^-$, (e) remaining 6-prong events.

Fig. 4 (a) Effective mass of slow proton plus π^+ for the (1, 5) events; there are 2 entries per event. A Δ^{++} signal is evident.
 (b) Effective mass of slow proton plus π^- for the (1, 5) events.

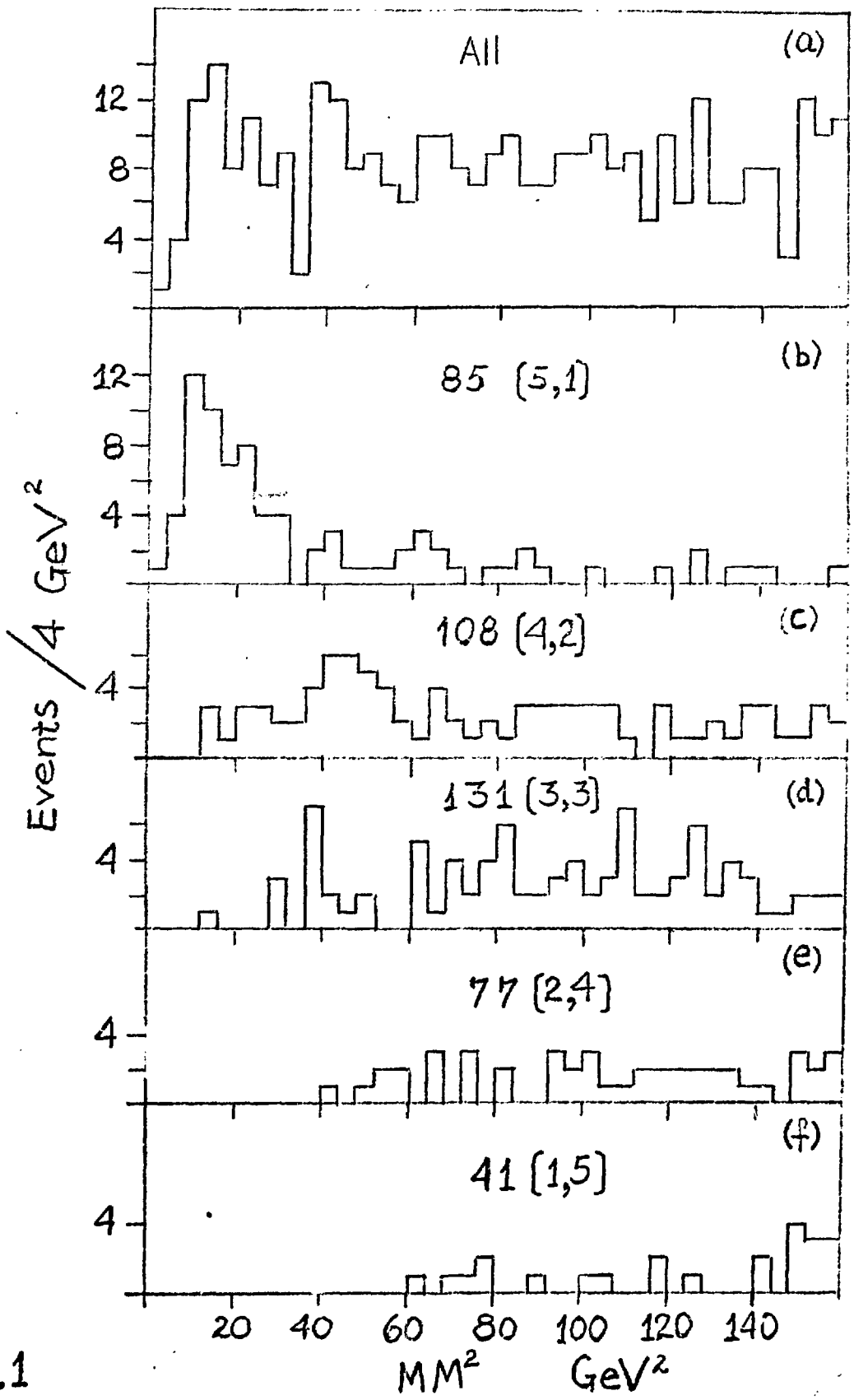


Fig.1

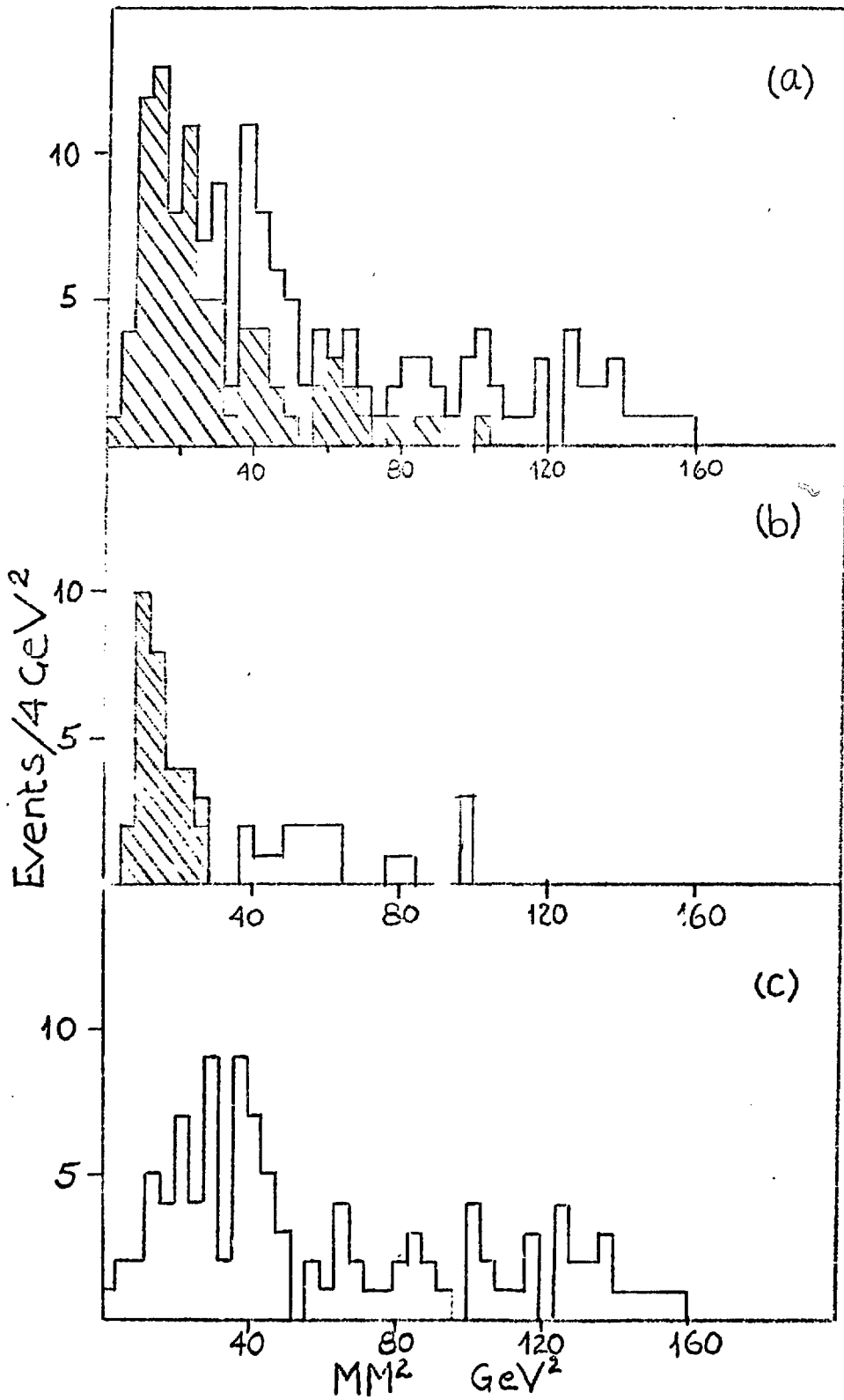


Fig. 2

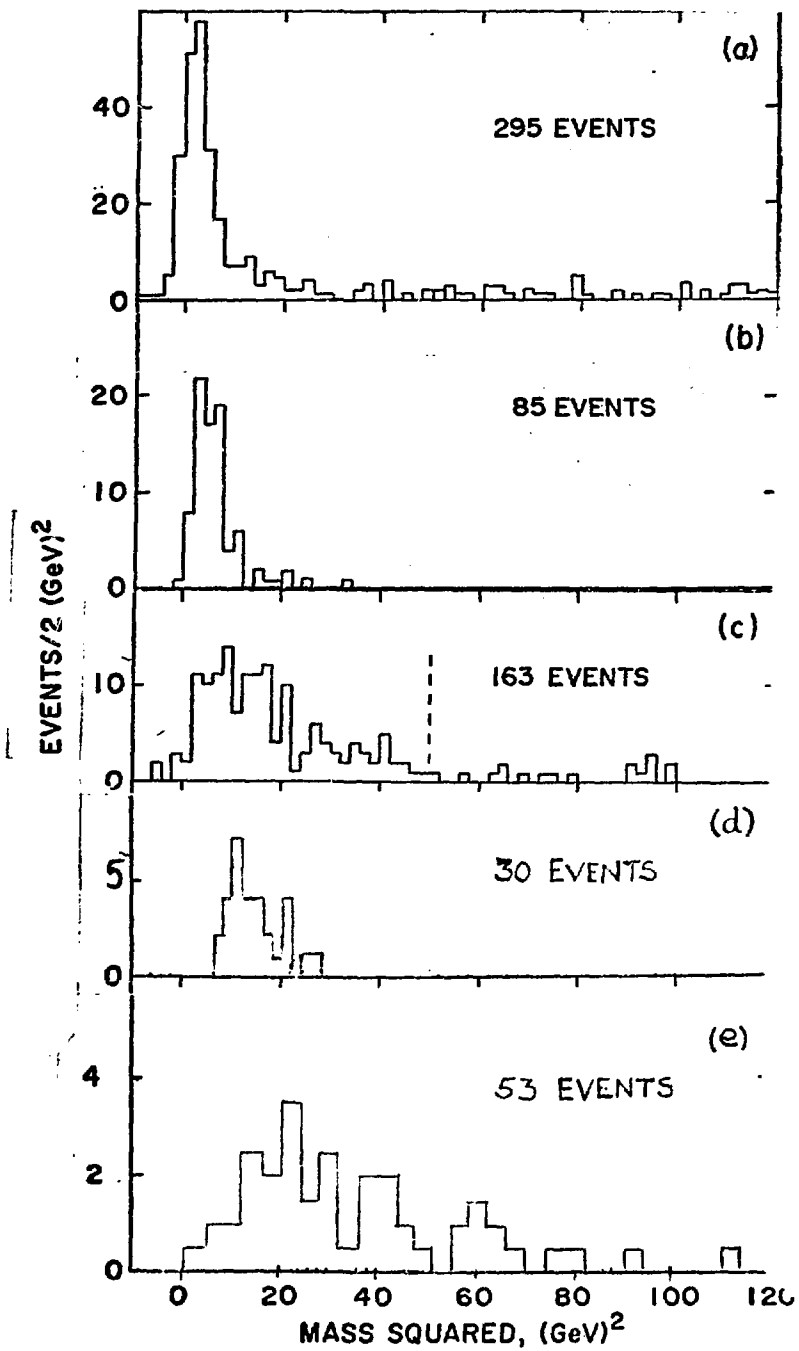


Fig. 3

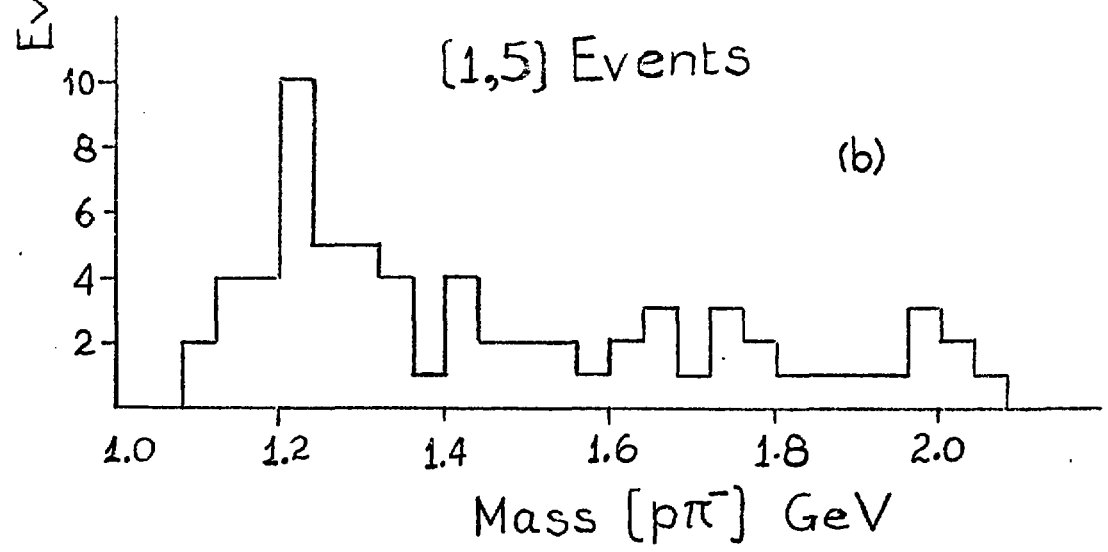
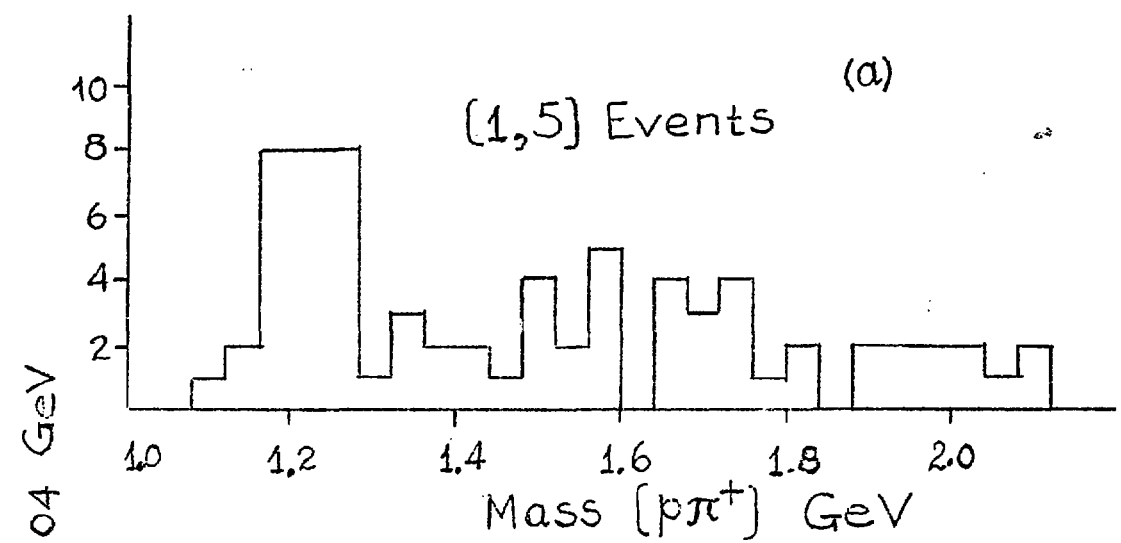


Fig. 4